Наносистеми, наноматеріали, нанотехнології
Nanosistemi, Nanomateriali, Nanotehnologii
2023, т. 21, № 3, сс. 583–592

PACS numbers: 65.80.-g, 68.37.Hk, 77.22.Ch, 77.80.Bh, 78.67.Bf, 81.07.Wx, 82.60.Qr

Size Effect of Submicron Barium-Titanate Particles on Its Phase Transitions and Dielectric Properties

A. R. Imamaliyev[1], I. R. Amiraslanov[1], F. F. Yahyayev[1], and A. A. Hadiyeva[2]

[1]*Institute of Physics,*
Ministry of Science and Education of the Republic of Azerbaijan,
131, H. Javid Ave.,
AZ1143 Baku, Azerbaijan
[2]*Azerbaijan State Oil and Industry University,*
20, Azadlig Str.,
AZ1010 Baku, Azerbaijan

The structure, dielectric properties, and phase transitions of ferroelectric barium-titanate ($BaTiO_3$) particles with sizes of 100, 200, 300, 400, and 500 nm are investigated by powder-diffractometry techniques, low-dimensional dielectric spectroscopy and differential scanning calorimetry (DSC), respectively. Analysis of the x-rays' diffraction spectra shows that, at room temperature for particles of all sizes, there are no signals corresponding to the cubic phase that contradicts the widely used core–shell model. As shown, the transition from cubic phase to tetragonal one shifts downward with a decrease in the $BaTiO_3$-particle size. For particles with a size of 100 nm, this shift is anomalously large and is of about 80°C. The cubic–tetragonal phase-transition enthalpy for these particles is higher by an order of magnitude in comparison with particles of other sizes. The peak corresponding to the tetragonal–orthorhombic transition is not found in the DSC thermogram in the case of 200 nm size particles. These particles are also distinguished by a significantly high value of the dielectric constant, which will make it possible to use these particles as the main component of superparaelectric materials in the future. The results are discussed to reconcile them with each other.

Структуру, діелектричні властивості та фазові переходи сеґнетоелектричних частинок барію титанату ($BaTiO_3$) розмірами у 100, 200, 300, 400 та 500 нм досліджено методами порошкової дифрактометрії, низькорозмірної діелектричної спектроскопії та диференційної сканувальної калориметрії (ДСК) відповідно. Аналіза спектрів дифракції Рентґенових променів показує, що за кімнатної температури для частинок будь-якого розміру відсутні сиґнали, які відповідають кубічній фазі, що су-

перечить широко використовуваному моделю ядро–оболонка. Показано, що перехід від кубічної фази до тетрагональної зміщується вниз зі зменшенням розміру частинок $BaTiO_3$. Для частинок розміром у 100 нм цей зсув аномально великий і становить близько 80°C. Ентальпія фазового переходу від кубічної фази до тетрагональної для цих частинок на порядок вище в порівнянні з частинками інших розмірів. Пік, що відповідає переходу з тетрагональної фази в орторомбічну, не виявляється в термограмі ДСК у випадку частинок розміром у 200 нм. Ці частинки також вирізняються значно високим значенням діелектричної проникности, що уможливить у майбутньому використовувати ці частинки в якості основного компонента суперпараелектричних матеріялів. Результати обговорюються, щоб узгодити їх один з одним.

Key words: barium titanate, ferroelectric, phase transition, dielectric permittivity.

Ключові слова: титанат барію, сеґнетоелектрик, фазовий перехід, діелектрична проникність.

(Received 14 January, 2023)

1. INTRODUCTION

The crystal of barium titanate ($BaTiO_3$), being a representative of perovskites, exhibits a strong ferroelectric property. The value of spontaneous polarization for the bulk sample at room temperature reaches 26 $\mu C/cm^2$ [1]. Due to this property, $BaTiO_3$ is widely used in various elements of electronic devices. These include nonlinear and supercapacitors, memory devices, infrared detectors, mechanical stress sensors, ultrasonic generators, *etc.* [2–4]. A thin film of barium titanate deposited on the silicon surface significantly increases the efficiency of solar cells, exhibiting light-trapping properties [5].

Recently, barium titanate-based nanocomposites made it possible to expand the application of this material. The main idea is that, by constructively combining the ferroelectric properties of $BaTiO_3$ with the properties of other functional materials, one can achieve high performance, and in some cases, obtain qualitatively new properties or effects [6, 7]. For example, barium titanate-based composites are used in energy and charge storage devices, multilayer capacitors, *etc.* [8–10].

In the last 20 years, the number of works devoted to liquid crystal-based nanocolloids has been rapidly growing. A summary of these works can be found in reviews [11–13]. The researchers hope that $BaTiO_3$ nanoparticles can be used in liquid crystal displays in the future since the addition of these particles to liquid crystal in a

tiny amount leads to tremendous improvements in the main electro-optical characteristics: lowering the threshold voltage and switching time.

In some cases, as noted above, qualitatively new effects arise [14–17]. A good example is the electromechanical effect with memory in the isotropic phase of liquid crystal [18].

To optimize the characteristics when using composites and colloidal systems based on submicron $BaTiO_3$ particles, it is necessary to find out how the structure and properties of these particles change in comparison with a bulk sample. For example, in Ref. [19], a core–shell model was proposed to explain the anomalous dielectric behaviour of the $BaTiO_3$ composite [20]. According to this model, submicron $BaTiO_3$ particles consist of a core with tetragonal symmetry and a thin shell with cubic symmetry. The thickness of the cubic shell, according to experimental data, is of 5–10 nm. Some works theoretically explain this model [21].

Another fundamental task when working with $BaTiO_3$-based composites and colloids is to establish the critical particle size, below which the ferroelectric property disappears. There is a great disagreement in the experimental data in this matter. It was stated in Ref. [22] that the spontaneous polarization of $BaTiO_3$ particles disappears at a size of 120 nm; in another study [23], it is considered that this size is equal to 10 nm. Analysing all previous works, Sedykh *et al.* [24] concluded that this discrepancy was associated with the method of obtaining $BaTiO_3$ particles, rather than with the difference in experimental methods.

To help eliminate the above uncertainties, in this work, the structure, dielectric properties, and phase transitions of $BaTiO_3$ particles with sizes of 100, 200, 300, 400, and 500 nm are studied by x-ray diffraction (XRD), low-frequency dielectric spectroscopy (LFDS) and differential scanning calorimetry (DSC) methods.

2. EXPERIMENT

Barium titanate particles were purchased from the US Nano Research Company. The image of these particles taken in a scanning electron microscope JOEL JSM-767F (Fig. 1, *a*–*e*) shows a good enough monodispersity of the samples.

The x-ray diffraction analysis of the samples was carried out in a Bruker D2-Phaser (CuK_α) diffractometer at the temperature of 22°C. The crystal lattice parameters were determined using the EVA and TOPAS programs by the Rietveld method [25]. These parameters were further corrected by using the LeBail refinement method [26].

To study the dielectric properties of the $BaTiO_3$ particles, they

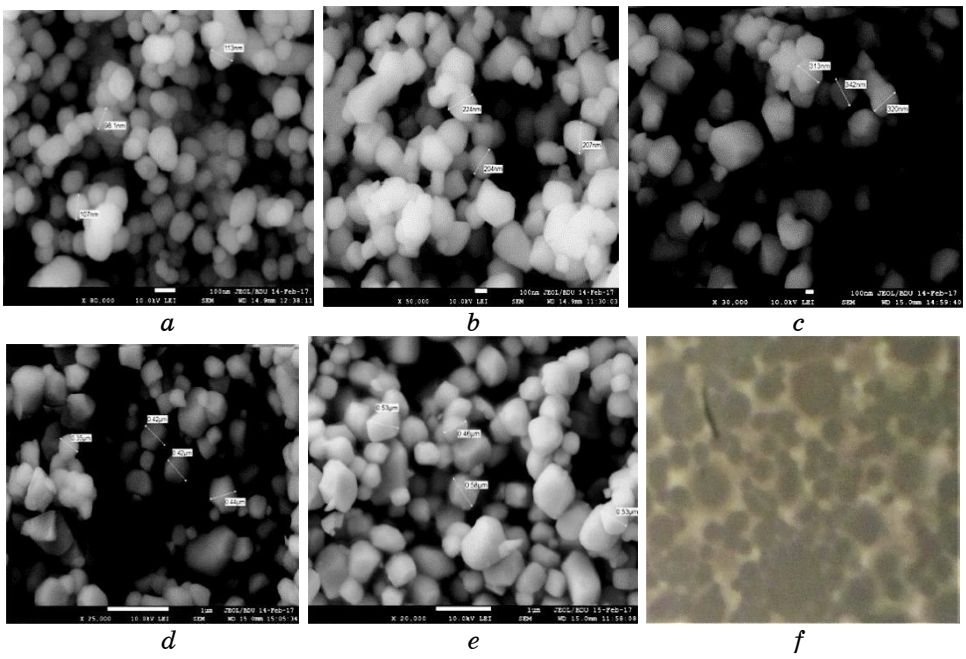

Fig. 1. *a*–*f*—view of $BaTiO_3$ particles in a scanning electron microscope, *e*—view of the mixture of oleic acid and 300 nm size $BaTiO_3$ particles in an optical microscope at ×1200 magnification.

were mixed with oleic acid. The volume fraction of particles of all sizes was of 43%. Figure 1, *e* shows the view of such a mixture in a microscope (Carl Zeiss Yena) at 1200-fold magnification. Before the measurement, the mixture was filled into a special cell. The cell consists of two plane–parallel glass plates, the inner surfaces of which are covered with a transparent conductive indium–tin oxide (ITO) layer. The thickness of the mixture in the cell was fixed with a teflon spacer. The dielectric permittivity (ε_m) of the mixture is determined by the electrical capacitance of the cell:

$$C = \varepsilon_0 \varepsilon \frac{s}{d}, \qquad (1)$$

$\varepsilon_0 = 8.85$ pF/m is the electric constant; $d = 30$ μm and $S = 1$ cm^2 are the thickness and the surface area of the sample, respectively.

The cell capacitance was measured in an LCR-meter IET 1920 in the frequency range of 20 Hz–1 MHz. The test signal amplitude was of 1 V.

The formula for heterogeneous mixtures was used to calculate the dielectric permittivity of $BaTiO_3$ particles from the dielectric permittivity of the mixture [27]:

$$\frac{\varepsilon_p - \varepsilon}{\varepsilon_p - \varepsilon_m}\left(\frac{\varepsilon_m}{\varepsilon}\right)^{1/3} = 1 - f\,; \qquad (2)$$

ε, ε_m, and ε_p are dielectric permittivities of the mixture, medium (oleic aside), and $BaTiO_3$ particles, respectively.

Phase transitions occurring in $BaTiO_3$ particles were investigated in a differential DSC NETZSCH Phoenix 204 F1 differential scanning calorimeter in the heating mode at the rate of 5°C/min.

3. RESULTS AND DISCUSSIONS

Figure 2 shows the diffraction spectra obtained from samples of $BaTiO_3$ with sizes of 100, 200, 300, 400, and 500 nm. The lattice parameters of samples refined using the LeBail refinement method [26] confirm that they belong to a tetragonal structure. The results are as follow: space group is $P4mm$, $a = 3.9944(1)$ Å, $c = 4.0362(2)$ Å, $v = 64.398(4)$ Å^3, $R_{\text{Bragg}} = 0.776\%$.

According to US NANO data, BT particles are characterized by a cubic system with sizes smaller than 100 nm. We see the absence of many maxima in particles with a size of 100 nm. This gives grounds to assume that these particles belong to the class of a cubic crystal. However, we were cautious about this thought and again analysed the situation. When comparing the full width corresponding to the half-height of the maxima (FWHM), we note that, for particles with a size of 100 nm, it has a greater value. The closeness of the values of the parameters a and c of the tetragonal lattice leads to the appearance of closely spaced groups of peaks

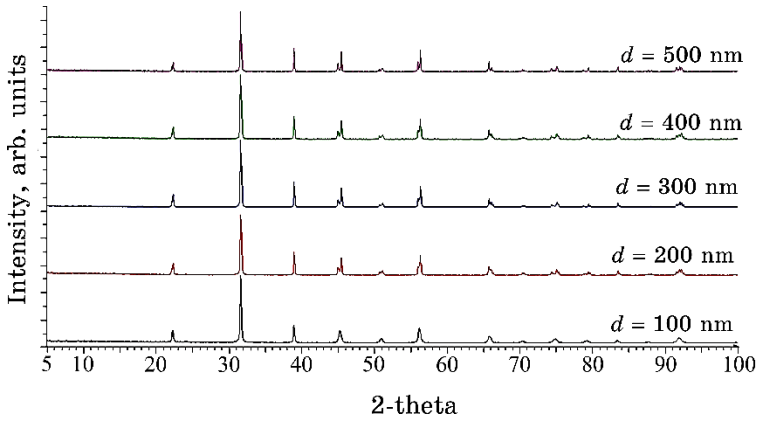

Fig. 2. Powder diffraction spectra obtained from samples of $BaTiO_3$ with various sizes.

($2\theta \cong 45°$, 51°, 56°, 66°, *etc.*) in the case of large $BaTiO_3$ particles. At the same time, we found that the total width of the peak groups in the case of large particles is equal to the width of the 100 nm-size particles. This means, in our opinion, the absence of a transition to the cubic phase. There is simply a decrease in the resolution in the spectrum due to the overlap of the broadened peaks in the groups in the case of particles with a size of 100 nm. Note once again that, if a transition to the cubic phase took place with a decrease in the size of $BaTiO_3$ particles, then, the group of peaks should have gathered into one point, as a result of which the width of the peaks in the spectrum of the 100 nm size particle should have been sharply reduced. In this case, the widths of all peaks should have been close to the width of a single peak $2\theta \cong 39°$, which we do not observe for 100 nm-size particles. Thus, at 22°C, the barium-titanate particles with the size of 100 nm also belong to the tetragonal class but probably with a lesser degree of perfection.

According to classical works [28], above 120°C, a bulk crystal of barium titanate possesses a cubic lattice exhibiting paraelectric property and, upon cooling below this temperature, it transforms into a tetragonal phase with a ferroelectric property. Upon further cooling just below room temperature (5–10°C), another modification occurs, the tetragonal lattice transitions to an orthorhombic lattice. At submicron sizes, these transitions can shift or even disappear due to the increasing role of surface effects [29, 30]. Thermograms taken in differential scanning calorimeter at different particle sizes are shown in Fig. 3. The smoothness of the curves corresponding to

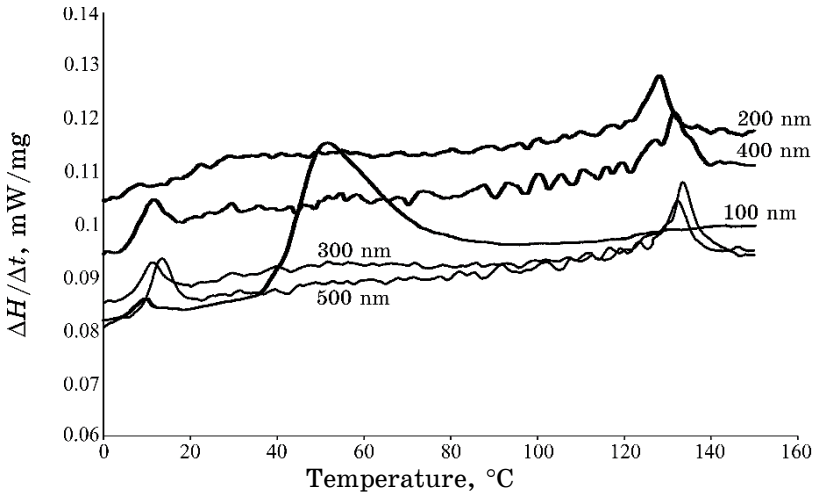

Fig. 3. DSC thermograms of $BaTiO_3$ at different particle sizes in heating mode.

large particles (400 nm and 500 nm) most likely is related to the rearrangement of the domain boundaries within these particles. The temperatures ($T_{o\,t}$ and $T_{t\,c}$) and enthalpies ($\Delta H_{o\,t}$ and $\Delta H_{t\,c}$) of the orthorhombic–tetragonal and tetragonal–cubic phase transitions were determined from these thermograms. The results are summarized in Table 1.

Figure 4 shows the frequency dependence of the real part of the dielectric permittivity of the mixtures of oleic and BT particles with different sizes.

TABLE 1.

Size of $BaTiO_3$ particles	100 nm	200 nm	300 nm	400 nm	500 nm
ΔH_{o-t}, J/g	0.098		0.222	0.261	0.362
T_{o-t}, °C	5.5		7.4	5.1	9.1
ΔH_{t-c}, J/g	4.273	0.341	0.391	0.495	0.493
T_{t-c}, °C	39.6	119.0	122.1	123.7	124.6

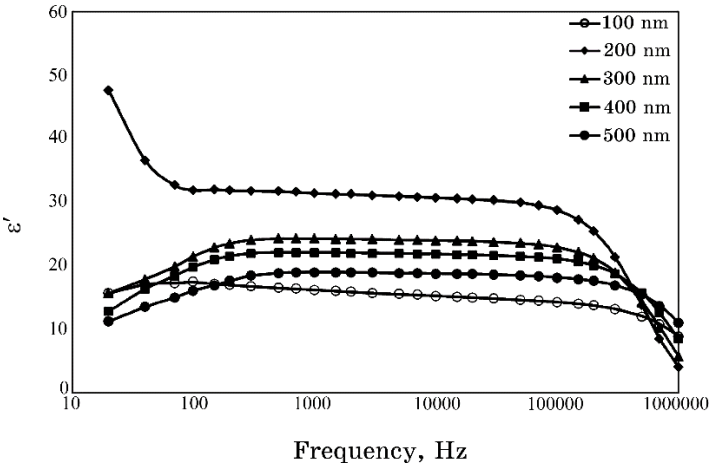

Fig. 4. Frequency dependence of the dielectric permittivity of the mixtures of oleic and $BaTiO_3$ particles with different sizes.

TABLE 2.

Size of particle	100 nm	200 nm	300 nm	400 nm	500 nm
Dielectric permittivity of mixtures	15.9	31.1	24.3	22.1	19.2
Dielectric permittivity of particles	67.4	911.2	223.5	158.3	108.8

Table 2 presents some important data extracted from these dependencies. The second row shows the dielectric constant of mixtures with barium titanate particles at 2 kHz. Using the formula (2) for effective dielectric permittivity of two-component heterogeneous systems, we can calculate the dielectric permittivity of BT particles with different sizes, which are shown in the third row of the table.

The most interesting results of DSC measurements are as follows. Small values of phase transition enthalpies show that both tetragonal–cubic and orthorhombic–tetragonal transitions are weak first-order transitions (the exceptions are 100 nm size particles). The temperature of the transition from tetragonal to cubic phase shifts downward with decreasing particle size. The magnitude of the shift is a few degrees, but for particles with a size of 100 nm, this shift is anomalously large and is approximately of 80°C. The enthalpy of the tetragonal–cubic phase transition for these particles is also higher by an order compared to other sizes. Another anomaly is related to 200 nm-size particles, for which the orthorhombic–tetragonal phase transition disappears (or is not observed, since DSC measurements are performed in the range from 0°C to 150°C).

Regarding dielectric measurements, the dielectric permittivity of particles increases with decreasing particle size, reaching a sharp maximum at 200 nm.

The small value of the dielectric permittivity of barium-titanate particles at a size of 100 nm is associated, as follows from a comparison of the experimental data, not with the disappearance, but with the weakening of the ferroelectric properties. This is confirmed by both x-ray data (at room temperature, these particles belong to the tetragonal class with a lesser degree of perfection) and DSC thermograms (transition from tetragonal phase to cubic phase takes place at 39°C).

As noted above, particles with a size of 200 nm attract attention with their high dielectric permittivity values. Similar results have been obtained before. For example, work by Wada *et al.* [19] found that, at the size of particles of 140 nm (in another paper, 58 nm [31]), the dielectric permittivity of $BaTiO_3$ particles takes the maximum value. The authors attributed this to the monodomain structure of $BaTiO_3$ particles. Most likely, the disappearance of the orthorhombic–tetragonal phase transition is also related to this phenomenon.

The presence of non-zero spontaneous polarization due to monodomain structure increases the value of free energy by $P_S^2/\left[2(\varepsilon-1)\varepsilon_0\right]$ (P_S is the spontaneous polarization of particles). In addition, this, in turn, leads to suppression of the orthorhombic–tetragonal phase transition or a strong shift in the transition to the low-temperature region.

4. CONCLUSION

The decrease in the size of submicron barium-titanate particles is reverberated through their structure and physical properties due to the increased role of the surface. This is confirmed by both x-ray studies and calorimetric and dielectric measurements. The most interesting results are obtained for particles with sizes of 100 nm and 200 nm: 1) a high value of dielectric permittivity and absence of orthorhombic–tetragonal phase transition for 200 nm size particles; 2) a sharp change in the temperature and heat of the ferroelectric transition from the tetragonal phase to the cubic one at a particle size of 100 nm. The first result, in our opinion, is related to the monodomain structure of these particles. Moreover, the second result is related to the deformation of the crystal structure of 100 nm-size particles.

REFERENCES

1. Karin M. Rabe, Matthew Dawber, Céline Lichtensteiger, Charles H. Ahn, and Jean-Marc Triscone, *Physics of Ferroelectrics: A Modern Perspective*, **105**: 1 (2007); https://doi.org/10.1007/978-3-540-34591-6_1
2. J. Scott, *Ferroelectric Materials for Energy Applications* (Wiley–VCH Verlag GmbH & Co. KGaA: 2018).
3. K. Uchino, *Ferroelectric Devices* (CRC Press: 2011).
4. Burcu Ertuğ, *American Journal of Engineering Research (AJER)*, **2**, No. 8: 1 (2013); https://www.ajer.org/papers/v2(8)/A0280107.pdf
5. A. K. Sharma, B. G. Priyadarshini, B. R. Mehta, and D. Kumar, *RSC Advances*, **5**: 59881(2015): https://doi.org/10.1039/C5RA07923C
6. Yu. Garbovskiy, O. Zribi, and A. Glushchenko, *Emerging Applications of Ferroelectric Nanoparticles in Materials Technologies, Biology and Medicine*, http://dx/doi/org/10.5772/52616
7. Markys G. Cain, *Characterisation of Ferroelectric Bulk Materials and Thin Films* (Springer: 2014).
8. K. P. Jayadevan and T. Y. Tseng, *Journal of Material Science: Materials of Electronics*, **3**, No. 8: 3439: (2002); https://doi.org/10.1023/A:1016129318548
9. S. Salemzadeh, A. Mellinger, and G. Caruntu, *ACS Applied Materials*, **20**, No. 6: 17506 (2014); http://dx/doi.org/10.1021/am502547h
10. P. N. Nikolarakis, I. A. Asimakopoulos, and L. Zoumpoulakis, *Journal of Nanomaterials*, Article ID 7023437: 1 (2018); https://doi.org/10.1155/2018/7023437
11. A. Glushchenko, Ch. Cohen, J. West, F. Li, E. Büyüktanır, and Y. Reznikov, *Molecular Crystals and Liquid Crystals*, **453**: 227 (2006); https://doi.org/10.1080/15421400600653852
12. Y. Reznikov, *Ferroelectric Colloids in Liquid Crystals: Chemistry, Physics, and Applications (Liquid Crystals Beyond Displays)* (Ed. Q. Li) (Hoboken, New Jersey: John Wiley & Sons, Inc.: 2012), p. 403.

13. Y. Reznikov, A. Glushchenko, and Y. Garbovskiy, *Ferromagnetic and Ferroelectric Nanoparticles in Liquid Crystals (Liquid Crystals with Nano and Microparticles* (Eds. J. Lagerwall and G. Scalia) (World Scientific Publishing: 2016), p. 657.
14. H.-H. Liang and J.-Y. Lee, *Enhanced Electro-Optical Properties of Liquid Crystals Devices by Doping with Ferroelectric Nanoparticles* (*Ferroelectrics—Material Aspects)* (Eds. M. Lallart) (Croatia: Intech Web. Org.: 2011), p. 193.
15. T. D. Ibragimov, A. R. Imamaliyev, and G. M. Bayramov, *Optik*, **127**: 1217 (2016); https://doi.org/ 10.1016/j.ijleo.2015.10.225
16. T. D. Ibragimov, A. R. Imamaliyev, and G. M. Bayramov, *Ferroelectrics*, **495**: 62 (2016): doi:10.1080/00150193.2016.1136732
17. A. R. Imamaliyev, Sh. A. Humbatov, and M. A. Ramazanov, *Beilstein Journal of Nanotechnology*, **9**: 824 (2018).
18. R. Basu, *Phys. Rev. E*, **89**: 022508 (2014); https://doi.org/10.1103/PhysRevE.89.022508
19. S. Wada, T. Hoshina, H. Yasuno, S.-M. Nam, H. Kakameto, H. Tsurumi, and M. Yashima, *Journal of Korean Physical Society*, **46**, No. 1: 303 (2005).
20. M. Anliker, H. R. Brugger, and W. Kanzig, *Helvetica Physica Acta*, **27**: 99 (1954).
21. C. Fang, D.X. Zhou, and Sh. P. Gong, *Physica B*, **406**: 1317 (2011); doi:10.1016/j.physb.2011.01.024
22. M. Tanaka and Y. Makino, *Ferroelectrics Lett.*, **24**: 13(1998); https://doi.org/10.1080/ 07315179808204451
23. K. Uchino, E. Sadanaga, and T. Hirose, *Journal of American Ceramic Society*, **72**: 1555 (1989).
24. P. Sedykh, D. Michel, E. Charnaya, and J. Haase, *Ferroelectrics*, **400**: 135 (2010); https://doi.org/10.1080/00150193.2010.505514
25. *Powder Diffraction: Theory and Practice* (Eds. R. E. Dinnebier and S. J. L. Billinge) (Cambridge: RSC Publisher: 2008).
26. V. K. Pecharsky and P. Y. Zavalij, *Fundamentals of Powder Diffraction and Structural Characterization of Materials* (Springer: 2022).
27. G. R. Gorur, *Dielectrics in the Electric Field* (CRC Press–Taylor and Francis Group: 2017).
28. Ch. Kittel, *Introduction to Solid State Physics* (John Willey and Sons Inc.: 2005).
29. K. Binder, *Ferroelectrics*, **73**: 43 (1987).
30. J. Yu and J. Chu, *Encyclopedia of Nanoscience and Nanotechnology* (Ed. H. S. Nalwa) (2004), vol. **6**, p. 389.
31. T. Hoshina, H. Yasuno, H. Kakameto, T. Tsurumi, and S. Wada, *Ferroelectrics*, **353**: 55 (2007); http://dx.doi.org/10.1080/00150190701367069